Power Electronics and Drives
Volume 4(39), 2019 DOI: 10.2478/pead-2019-0013

sciendo

Power Electronics and Drives

Non-Cartesian Frame Transformation-Based Control of a Three-Phase Power Converter During Unbalanced Voltage Dip – Part I: Transformation Principles

Research Article

Grzegorz Iwański, Paweł Maciejewski, Tomasz Łuszczyk

Warsaw University of Technology, Institute of Control and Industrial Electronics, ul. Koszykowa 75, 00-662 Warszawa, Poland

Received March 04, 2019; Accepted July 09, 2019

Abstract: One of the currently investigated problems in power electronics-based electrical energy conversion is proper operation of electronic converters during grid voltage imbalance and harmonics. In classic control methods, it introduces oscillations of variables, resulting in the necessity to improve control systems with signals filtration and usually by application of resonant terms as part of current controllers. The paper presents a new approach to grid-connected inverter control based on transformation to a non-Cartesian frame, the parameters of which are correlated with grid voltage asymmetry. The proposed method results in resignation from resonant terms used as controllers and their replacement with proportional–integral terms for which anti-wind-up structures are significantly simpler than for oscillatory terms. The paper presents new transformation principles, features and some simulation results showing the waveforms of signals transformed to the new non-Cartesian frame.

Keywords: *AC–DC power conversion • current control • Clarke's transformation*

1. Introduction

The number of grid-connected inverters has significantly grown in the recent years. Increased costs in the case of rectifier operation in relation to passive diode rectifiers are compensated for by increased capabilities of harmonics content reduction and reactive power management. In the case of unbalanced grid operation, it enables negative-sequence management, impossible in passive rectifiers. In the case of renewable energy sources integration, the interfacing converters increase conversion efficiency of variable speed generators, whereas in photovoltaic sources and battery energy storage systems, grid side converters are anyway necessary to integrate them with an AC power network.

Recently, interconnection requirements called grid codes have been established and they are more and more restrictive. Large emphasis in these standards is put on assistance of converters during voltage sags, to increase stability of the power distribution system (Abdeltawab and Mohamed, 2016). In order to control a power converter connected to an asymmetrical grid, different methods have been developed. The most popular are positive and negative-sequence decomposition-based control for management of positive and negative-sequence components in different coordinate frames (Cheng and Nian, 2016; Guo et al., 2017, 2018; Nian et al., 2015) and resonant controllers of the fundamental harmonics component (common for positive and negative sequences) (Guo et al., 2018). Methods based on calculating the reference signal matching the desired control target, without positive- and negative-sequence decomposition, are also found in the literature (Iwanski, 2019; Iwanski et al., 2017). Usually, they

* *Email: iwanskig@isep.pw.edu.pl, pawel.maciejewski@ee.pw.edu.pl, tomasz.luszczyk@ee.pw.edu.pl*

require oscillatory terms to track the reference current including a 50-Hz frequency component if controlled in the stationary $\alpha\beta$ frame or constant and a 100-Hz component if controlled in a rotating synchronously dq reference frame.

Although implementation of oscillatory terms in a digital signal processor is not complicated and obtained results are usually satisfactory, the publications rarely discuss the problems of gains tuning and anti-wind-up structures of oscillatory terms. Especially, tuning of controller built with oscillatory terms is not a trivial problem and in a classic way cannot assure stability in all conditions. To do it honestly, a linear quadratic LQ optimization method has been investigated (Gałecki et al., 2016) and combined with particle swarm optimization method (Gałecki et al., 2018). It makes the control system expanded and requires significant experience from the control system designer, whereas the control plant is relatively simple.

This paper presents a new approach based on transformation to the non-Cartesian frame. The main idea of this concept is to establish a new coordinate system, in which oscillations of controlled variables in the dq frame during an asymmetrical voltage dip and/or asymmetrical reference current do not exist. It can be done by estimating amplitude and phase of each voltage component in a natural $\alpha\beta$ frame and adjusting the newly proposed transformation to match a new reference. By choosing different combinations of the calculated amplitude multipliers and phase shifts, different control objectives can be achieved. Although an approach based on $\alpha\beta$ components' magnitudes and phase shift calculation can be found in the literature (Rizo et al., 2012), its application is limited to saturation of controllers. This approach is not related to current control and reference current calculation or to the analysis of different control targets such as current imbalance corresponding or opposite to grid voltage imbalance and symmetrical current target.

A similar concept to the proposed one is known in post-fault operation of multiphase machines (Abdel-Khalik et al., 2018; Levi et al., 2007). The difference is that in the case of multiphase machines, the new reference frame can be calculated offline for each phase fault and mapped in a table, due to the fixed position of stator phase windings. For a grid-connected converter, estimation of new transformation parameters has to be done online, because during a voltage dip, phase displacement and voltage amplitude reduction (Rizo et al., 2012) depend on the type and depth of grid voltage dip. To do so, the second-order generalized integrator (SOGI) (Patiño et al., 2015; Rodriguez et al., 2011; Xin et al., 2016) was chosen as a phasor estimator because of its robustness, convergence speed and low computational intensity. This paper presents an analysis of the newly developed non-Cartesian frame transformation and some simulations proving the theory of transformation.

2. The Principles of the Proposed Non-Cartesian Frame Transformation

Clarke's transformation (Clarke, 1943) allows to represent a three-phase system in the form of two orthogonal components of the vector of voltage, current or flux. In case of symmetrical sinusoidal three-phase signals, α and β components of the vector in a natural $\alpha\beta$ frame are represented by the following equation:

$$\begin{bmatrix} x_\alpha \\ x_\beta \end{bmatrix} = \begin{bmatrix} |x| cos(\theta) \\ |x| sin(\theta) \end{bmatrix} \tag{1}$$

where x represents vector of voltage, current or flux and θ represents the vector rotation angle, which changes according to the pulsation ω of three-phase signals as represented by the following equation:

$$\theta = \int_{t_0}^{t} \omega(\tau) d\tau + \theta_0 \tag{2}$$

Park's transformation (Park, 1929) is the foundation of vector control algorithms in power electronics and drives. It allows representation of vector x in the frame, in which vector x has constant components. There are several reasons for using this transformation, mainly linearization of the control system, constant reference signals and consequently implementation of classic proportional–integral controllers eliminating steady-state errors for constant control variables. There is an infinite number of frames in which vector x obtains constant components. Usually a specific one is selected that is oriented to the d component of the reference vector (e.g., flux in the field-oriented

control of electric machines or grid voltage vector in voltage oriented control of grid side converters). Classic rotation transformation for synchronization with the d component of the vector can be described as follows:

$$\begin{bmatrix} x_d \\ x_q \end{bmatrix} = \begin{bmatrix} cos(\theta) & sin(\theta) \\ -sin(\theta) & cos(\theta) \end{bmatrix} \begin{bmatrix} x_\alpha \\ x_\beta \end{bmatrix} = \begin{bmatrix} cos(\theta) & sin(\theta) \\ -sin(\theta) & cos(\theta) \end{bmatrix} \begin{bmatrix} |x|cos(\theta) \\ |x|sin(\theta) \end{bmatrix} = \begin{bmatrix} |x| \\ 0 \end{bmatrix} \tag{3}$$

In the case in which the analyzed vector contains both positive and negative sequence, the instantaneous values of x_α and x_β vector components in the $\alpha\beta$ frame can be represented by the following equation:

$$\begin{bmatrix} x_\alpha \\ x_\beta \end{bmatrix} = \begin{bmatrix} |x_\alpha| cos(\theta_s - \theta_\alpha) \\ |x_\beta| cos(\theta_s - \theta_\beta) \end{bmatrix} \tag{4}$$

where $|x_\alpha|$ and $|x_\beta|$ are the amplitudes of the x_α and x_β components, respectively, and θ_α and θ_β are the phase shifts between $\alpha\beta$ component signals and positive sequence α component signal, respectively. Vector instantaneous angular speed ω in (2) is not constant when an imbalance occurs but contains double-grid frequency oscillations. Similarly, vector length $|x|$ in (1) contains double-grid frequency oscillations. Thus, the $\alpha\beta$ to dq transformation angle θ (2) is changed to θ_s according to constant angular speed ω_s (5) of the reference frame synchronized with a positive sequence vector. This is to obtain synchronous operation with a dominating positive sequence component, and the new angle is usually obtained from the phase-locked loop PLL structures or other synchronization methods.

$$\theta_s = \int_{t_0}^{t} \omega_s(\tau) d\tau + \theta_{s0} \tag{5}$$

The transformation of asymmetrical $\alpha\beta$ components to the frame rotating synchronously with a positive sequence vector component is represented by the following equation:

$$\begin{bmatrix} x_d \\ x_q \end{bmatrix} = \begin{bmatrix} cos(\theta_s) & sin(\theta_s) \\ -sin(\theta_s) & cos(\theta_s) \end{bmatrix} \begin{bmatrix} x_\alpha \\ x_\beta \end{bmatrix} = \begin{bmatrix} cos(\theta_s) & sin(\theta_s) \\ -sin(\theta_s) & cos(\theta_s) \end{bmatrix} \begin{bmatrix} |x_\alpha| cos(\theta_s - \theta_\alpha) \\ |x_\beta| cos(\theta_s - \theta_\beta) \end{bmatrix} \tag{6}$$

The dq classic frame rotates synchronously with a positive sequence vector component, whereas the vector contains both positive and negative sequences. Thus, x_d and x_q components of the vector contain constant components and double-grid frequency oscillatory terms. Transformation (6) provides the following form of vector components:

$$\begin{aligned} \begin{bmatrix} x_d \\ x_q \end{bmatrix} &= \begin{bmatrix} cos(\theta_s) & sin(\theta_s) \\ -sin(\theta_s) & cos(\theta_s) \end{bmatrix} \begin{bmatrix} |x_\alpha| cos(\theta_s - \theta_\alpha) \\ |x_\beta| cos(\theta_s - \theta_\beta) \end{bmatrix} \\ &= \begin{bmatrix} |x_\alpha| cos(\theta_s) cos(\theta_s - \theta_\alpha) + |x_\beta| sin(\theta_s) cos(\theta_s - \theta_\beta) \\ -|x_\alpha| sin(\theta_s) cos(\theta_s - \theta_\alpha) + |x_\beta| cos(\theta_s) cos(\theta_s - \theta_\beta) \end{bmatrix} \\ &= \frac{1}{2} \begin{bmatrix} |x_\alpha| \left(cos(\theta_\alpha) + cos(2\theta_s - \theta_\alpha) \right) + |x_\beta| \left(sin(2\theta_s - \theta_\beta) + sin(\theta_\beta) \right) \\ |x_\alpha| \left(-sin(2\theta_s - \theta_\alpha) - sin(\theta_\alpha) \right) + |x_\beta| \left(cos(\theta_\beta) + cos(2\theta_s - \theta_\beta) \right) \end{bmatrix} \end{aligned} \tag{7}$$

Transformation angle θ_s changes in time according to (5), and when $|x_\alpha|$ and $|x_\beta|$ differ, $\theta_\beta - \theta_\alpha = \theta_{\beta\alpha} \neq \pi/2$ or both, negative-sequence component occurs, and x_d or x_q component contains oscillatory terms with double-grid frequency.

Let us introduce a new transformation from the natural $\alpha\beta$ frame to the new $\alpha'\beta'$ stationary frame, in which additional angles θ'_α and θ'_β are taken into consideration as phase shifts of non-Cartesian coordinates frame $\alpha'\beta'$

axes (both in relation to the α axis of the natural $\alpha\beta$ frame). A corresponding vector diagram with both natural $\alpha\beta$ and new non-Cartesian $\alpha'\beta'$ frames is shown in Fig. 1.

Derivation of $\alpha\beta$ to $\alpha'\beta'$ transformation is as follows:

$$|BC| = x_\beta \frac{cos(\theta'_\beta)}{sin(\theta'_\beta)} \qquad (8)$$
$$|EF| = x_\alpha \frac{sin(\theta'_\alpha)}{cos(\theta'_\alpha)}$$

$$|AB| = x_\alpha - |BC| = x_\alpha - x_\beta \frac{cos(\theta'_\beta)}{sin(\theta'_\beta)} \qquad (9)$$
$$|AE| = x_\beta - |EF| = x_\beta - x_\alpha \frac{sin(\theta'_\alpha)}{cos(\theta'_\alpha)}$$

Using the law of sines, we get

$$\frac{|AB|}{sin(\theta'_{\beta\alpha})} = \frac{x'_\alpha}{sin(\pi - \theta'_\beta)} = \frac{x'_\alpha}{sin(\theta'_\beta)} \qquad (10)$$
$$\frac{|AE|}{sin(\theta'_{\beta\alpha})} = \frac{x'_\beta}{sin\left(\frac{\pi}{2} + \theta'_\alpha\right)} = \frac{x'_\beta}{cos(\theta'_\alpha)}$$

Thus,

$$x'_\alpha = \frac{|AB| sin(\theta'_\beta)}{sin(\theta'_{\beta\alpha})} = \frac{\left(x_\alpha - x_\beta \frac{cos(\theta'_\beta)}{sin(\theta'_\beta)}\right) sin(\theta'_\beta)}{sin(\theta'_{\beta\alpha})} = \frac{x_\alpha sin(\theta'_\beta) - x_\beta cos(\theta'_\beta)}{sin(\theta'_{\beta\alpha})} \qquad (11)$$
$$x'_\beta = \frac{|AE| cos(\theta'_\alpha)}{sin(\theta'_{\beta\alpha})} = \frac{\left(x_\beta - x_\alpha \frac{sin(\theta'_\alpha)}{cos(\theta'_\alpha)}\right) cos(\theta'_\alpha)}{sin(\theta'_{\beta\alpha})} = \frac{-x_\alpha sin(\theta'_\alpha) + x_\beta cos(\theta'_\alpha)}{sin(\theta'_{\beta\alpha})}$$

The transformation from $\alpha\beta$ to $\alpha'\beta'$ takes the following form:

$$\begin{bmatrix} x'_\alpha \\ x'_\beta \end{bmatrix} = \frac{1}{sin(\theta'_{\beta\alpha})} \begin{bmatrix} sin(\theta'_\beta) & -cos(\theta'_\beta) \\ -sin(\theta'_\alpha) & cos(\theta'_\alpha) \end{bmatrix} \begin{bmatrix} x_\alpha \\ x_\beta \end{bmatrix} \qquad (12)$$

Let us take into account that the new axis α' has the position of the positive sequence vector x_p, for which the x_α component of vector x has the maximum value x_α^{max} (equal to its amplitude $|x_\alpha|$). Analogously, the β' axis has the position of a positive sequence vector x_p, in which the x_β component has the maximum value $x_\beta^{max} = |x_\beta|$.

Fig. 2 presents the vector diagram of instantaneous cases, when the x vector lies in the positions giving maximum x_α and x_β components in the classic $\alpha\beta$ frame. In a new $\alpha'\beta'$ frame, when the sinusoidal signal x'_α reaches the

maximum or minimum value, x'_β reaches zero. Thus, the x'_α and x'_β signals are shifted by $\pi/2$, but they may have different amplitudes depending on the type of imbalance. Let us assign the θ'_α and θ'_β angles and prove that the selected angles of new axes make the vector x projection to the α axis become correlated with vector x projection to the new α' axis, and vector x projection to the β axis become correlated with vector x projection to the new β' axis. The correlation is that when the x_p position overlaps with the α axis, the x'_α has the maximum value, and when the x_p vector overlaps with the θ'_α position, the x vector projection to the α axis (x_α component) has the maximum value (Fig. 2a). Analogously, when the x_p position overlaps with the β axis, the x'_β has the maximum value, and when the x_p vector overlaps with the θ'_β position, the x vector projection to the β axis (x_β component) has the maximum value (Fig. 2b).

When the positive sequence vector x_p lies along the α axis, the position of vector x can be described by the following equation:

$$tg\left(\theta'_\alpha\right)=\boxed{\frac{sin\left(\theta'_\alpha\right)}{cos\left(\theta'_\alpha\right)}=\frac{\left|x_n\right|sin\left(\theta_n\right)}{\left|x_p\right|+\left|x_n\right|cos\left(\theta_n\right)}\frac{x'_\alpha}{x'_\alpha}} \tag{13}$$

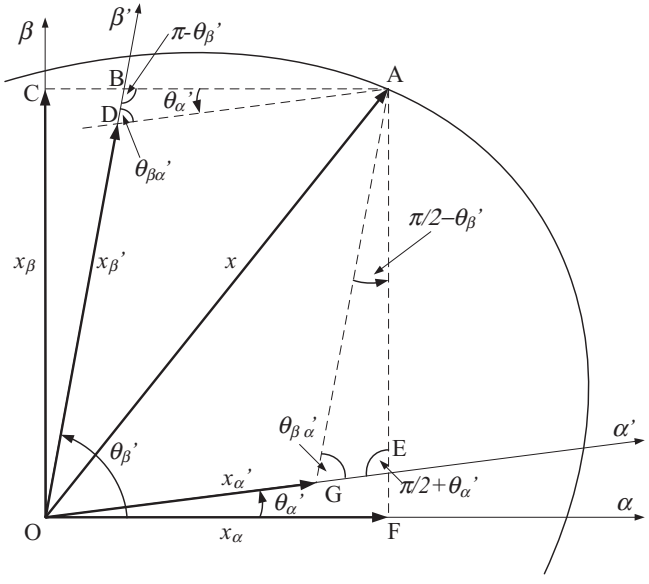

Fig. 1. Vector diagram presenting the natural $\alpha\beta$ stationary frame and non-Cartesian $\alpha'\beta'$ frame with axes positions θ'_α and θ'_β adjusted to three-phase signal imbalance and vector projections.

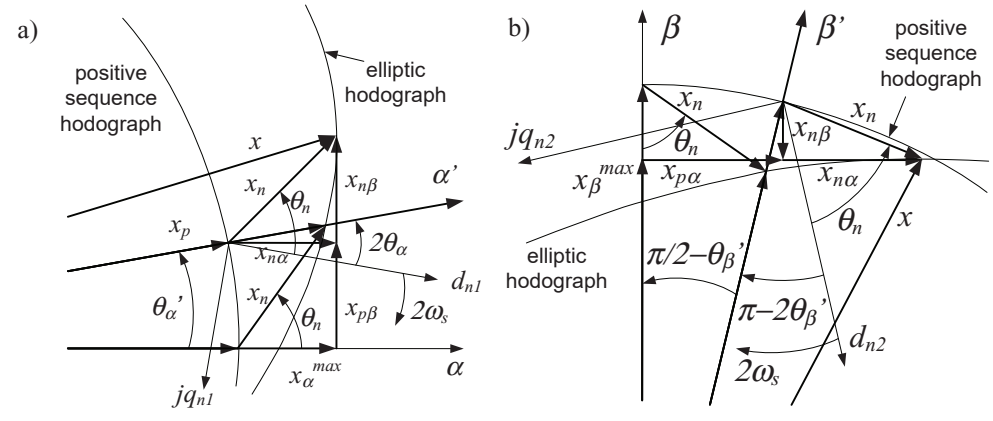

Fig. 2. Diagram presenting relations between vector projections when $\alpha'\beta'$ axes are adjusted to three-phase signal imbalance, a) vector projections to the α and α' axes, b) vector projections to the β and β' axes.

The x_α component can be described as follows:

$$x_\alpha = |x_p| cos(\theta_s) + |x_n| cos(\theta_n - \theta_s) \tag{14}$$

We can write that

$$x_\alpha = x_\alpha^{max} if \ \frac{dx_\alpha}{d\theta_s} = 0 \tag{15}$$

Thus,

$$\frac{d}{d\theta_s}\left(|x_p| cos(\theta_s) + |x_n| cos(\theta_n - \theta_s)\right) = -|x_p| sin(\theta_s) + |x_n| sin(\theta_n - \theta_s) = 0 \tag{16}$$

It can be derived that

$$tg(\theta_s) = \frac{sin(\theta_s)}{cos(\theta_s)} = \frac{|x_n| sin(\theta_n)}{|x_p| + |x_n| cos(\theta_n)} \tag{17}$$

It corresponds to (13) for $\theta_s = \theta'_\alpha$.

For θ'_β angle, a similar derivation can be made:

$$tg\left(\frac{\pi}{2} - \theta'_\beta\right) = \frac{sin\left(\frac{\pi}{2} - \theta'_\beta\right)}{cos\left(\frac{\pi}{2} - \theta'_\beta\right)} = \boxed{\frac{cos(\theta'_\beta)}{sin(\theta'_\beta)} = \frac{|x_n| sin(\theta_n)}{|x_p| - |x_n| cos(\theta_n)} \frac{x'_\beta}{x'_\beta}} \tag{18}$$

$$x_\beta = |x_p| sin(\theta_s) + |x_n| sin(\theta_n - \theta_s) \tag{19}$$

$$x_\beta = x_\beta^{max} if \ \frac{dx_\beta}{d\theta_s} = 0 \tag{20}$$

$$\frac{d}{d\theta_s}\left(|x_p| sin(\theta_s) + |x_n| sin(\theta_n - \theta_s)\right) = |x_p| cos(\theta_s) - |x_n| cos(\theta_n - \theta_s) = 0 \tag{21}$$

from which the following equation can be derived:

$$\frac{cos(\theta_s)}{sin(\theta_s)} = \frac{|x_n| sin(\theta_n)}{|x_p| - |x_n| cos(\theta_n)} \tag{22}$$

It corresponds to (18) for $\theta_s = \theta'_\beta$.

Noting this, it must be proved additionally that the θ'_α position of the vector x provides the maximum value of the x'_α projected component and the θ'_β position of the vector x provides the maximum value of the x'_β projected component. Inserting (14) and (19) into (11), we can describe vector components in a new $\alpha'\beta'$ frame as given in the following equation:

$$x'_\alpha = \frac{\left(|x_p| cos(\theta_s) + |x_n| cos(\theta_n - \theta_s)\right) sin(\theta'_\beta) - \left(|x_p| sin(\theta_s) + |x_n| sin(\theta_n - \theta_s)\right) cos(\theta'_\beta)}{sin(\theta'_{\beta\alpha})}$$

$$x'_\beta = \frac{\left(-|x_p| cos(\theta_s) - |x_n| cos(\theta_n - \theta_s)\right) sin(\theta'_\alpha) + \left(|x_p| sin(\theta_s) + |x_n| sin(\theta_n - \theta_s)\right) cos(\theta'_\alpha)}{sin(\theta'_{\beta\alpha})} \tag{23}$$

Noting that

$$\begin{cases} x'_\alpha = x_\alpha^{max'} \; if \; \dfrac{dx'_\alpha}{d\theta_s} = 0 \\ x'_\beta = x_\beta^{max'} \; if \; \dfrac{dx'_\beta}{d\theta_s} = 0 \end{cases} \tag{24}$$

we obtain (25ab)

$$\frac{dx'_\alpha}{d\theta_s} = \frac{1}{sin\left(\theta'_{\beta\alpha}\right)} \frac{d}{d\theta_s} \left(\left(\left| x_p \right| cos\left(\theta_s\right) + \left| x_n \right| cos\left(\theta_n - \theta_s\right) \right) sin\left(\theta'_\beta\right) - \left(\left| x_p \right| sin\left(\theta_s\right) + \left| x_n \right| sin\left(\theta_n - \theta_s\right) \right) cos\left(\theta'_\beta\right) \right) \tag{25a}$$

$$= \frac{1}{sin\left(\theta'_{\beta\alpha}\right)} \left(-\left| x_p \right| sin\left(\theta_s\right) sin\left(\theta'_\beta\right) + \left| x_n \right| sin\left(\theta_n - \theta_s\right) sin\left(\theta'_\beta\right) - \left| x_p \right| cos\left(\theta_s\right) cos\left(\theta'_\beta\right) + \left| x_n \right| cos\left(\theta_n - \theta_s\right) cos\left(\theta'_\beta\right) \right)$$

$$\frac{dx'_\beta}{d\theta_s} = \frac{1}{sin\left(\theta'_{\beta\alpha}\right)} \frac{d}{d\theta_s} \left(\left(-\left| x_p \right| cos\left(\theta_s\right) - \left| x_n \right| cos\left(\theta_n - \theta_s\right) \right) sin\left(\theta'_\alpha\right) + \left(\left| x_p \right| sin\left(\theta_s\right) + \left| x_n \right| sin\left(\theta_n - \theta_s\right) \right) cos\left(\theta'_\alpha\right) \right) \tag{25b}$$

$$= \frac{1}{sin\left(\theta'_{\beta\alpha}\right)} \left(\left| x_p \right| sin\left(\theta_s\right) sin\left(\theta'_\alpha\right) - \left| x_n \right| sin\left(\theta_n - \theta_s\right) sin\left(\theta'_\alpha\right) + \left| x_p \right| cos\left(\theta_s\right) cos\left(\theta'_\alpha\right) - \left| x_n \right| cos\left(\theta_n - \theta_s\right) cos\left(\theta'_\alpha\right) \right)$$

Taking into account (13) and (18), after derivation of (25a) and (25b), respectively, it can be written that

$$\frac{dx'_\alpha}{d\theta_s} = \frac{1}{\left| x'_\beta \right| sin\left(\theta'_{\beta\alpha}\right)} \left(-\left| x_p \right| sin\left(\theta_s\right) \left(\left| x_p \right| - \left| x_n \right| cos\left(\theta_n\right) \right) + \left| x_n \right| sin\left(\theta_n - \theta_s\right) \left(\left| x_p \right| - \left| x_n \right| cos\left(\theta_n\right) \right) \right. \tag{26a}$$

$$\left. - \left| x_p \right| cos\left(\theta_s\right) \left| x_n \right| sin\left(\theta_n\right) + \left| x_n \right| cos\left(\theta_n - \theta_s\right) \left| x_n \right| sin\left(\theta_n\right) \right) = - \frac{\left(\left| x_p \right|^2 - \left| x_n \right|^2 \right) sin\left(\theta_s\right)}{\left| x'_\beta \right| sin\left(\theta'_{\beta\alpha}\right)}$$

$$\frac{dx'_\beta}{d\theta_s} = \frac{1}{\left| x'_\alpha \right| sin\left(\theta'_{\beta\alpha}\right)} \tag{26b}$$

$$\left(\left| x_p \right| sin(\theta_s) \left| x_n \right| sin(\theta_n) - \left| x_n \right| sin(\theta_n - \theta_s) \left| x_n \right| sin(\theta_n) \right.$$

$$\left. + \left| x_p \right| cos(\theta_s) \left(\left| x_p \right| + \left| x_n \right| cos(\theta_n) \right) - \left| x_n \right| cos(\theta_n - \theta_s) \left(\left| x_p \right| + \left| x_n \right| cos(\theta_n) \right) \right)$$

$$= \frac{\left(\left| x_p \right|^2 - \left| x_n \right|^2 \right) cos\left(\theta_s\right)}{\left| x'_\alpha \right| sin\left(\theta'_{\beta\alpha}\right)}$$

Finally, it can be concluded that

$$\frac{dx'_\alpha}{d\theta_s} = 0 \; if \; \theta_s = 0$$

$$\frac{dx'_\beta}{d\theta_s} = 0 \; if \; \theta_s = \pi / 2 \tag{27}$$

which according to Fig. 2 means that the x'_α projection of the x vector component has the maximum value when the synchronous angle θ_s is zero (positive sequence vector x_p overlaps with the α axis of the natural $\alpha\beta$ frame) and the x'_β projection of the x vector component has the maximum value when the synchronous angle θ_s equals $\pi/2$ (positive sequence vector x_p overlaps with the β axis of the natural $\alpha\beta$ frame).

The amplitudes of x'_α and x'_β components, respectively, are equal to

$$\left|x'_\alpha\right| = \sqrt{\left(\left|x_p\right| + \left|x_n\right| cos\left(\theta_n\right)\right)^2 + \left(\left|x_n\right| sin\left(\theta_n\right)\right)^2} = \sqrt{\left|x_p\right|^2 + \left|x_n\right|^2 + 2\left|x_p\right|\left|x_n\right| cos\left(\theta_n\right)} \tag{28a}$$

$$\left|x'_\beta\right| = \sqrt{\left(\left|x_p\right| - \left|x_n\right| cos\left(\theta_n\right)\right)^2 + \left(\left|x_n\right| sin\left(\theta_n\right)\right)^2} = \sqrt{\left|x_p\right|^2 + \left|x_n\right|^2 - 2\left|x_p\right|\left|x_n\right| cos\left(\theta_n\right)} \tag{28b}$$

Simultaneously, taking into account (13), (18) and (28ab), the amplitudes of x_α and x_β components are equal to the amplitudes of x'_α and x'_β, respectively:

$$\begin{aligned}\left|x_\alpha\right| &= \left|x_p\right| cos\left(\theta'_\alpha\right) + \left|x_n\right| cos\left(\theta_n - \theta'_\alpha\right) = \left|x_p\right| \frac{\left|x_p\right| + \left|x_n\right| cos\left(\theta_n\right)}{\left|x'_\alpha\right|} + \left|x_n\right| cos\left(\theta_n\right) \frac{\left|x_p\right| + \left|x_n\right| cos\left(\theta_n\right)}{\left|x'_\alpha\right|} \\ &+ \left|x_n\right| sin\left(\theta_n\right) \frac{\left|x_n\right| sin\left(\theta_n\right)}{\left|x'_\alpha\right|} = \frac{\left|x_p\right|^2 + \left|x_n\right|^2 + 2\left|x_p\right|\left|x_n\right| cos\left(\theta_n\right)}{\left|x'_\alpha\right|} = \left|x'_\alpha\right|\end{aligned} \tag{29a}$$

$$\begin{aligned}\left|x_\beta\right| &= \left|x_p\right| sin\left(\theta'_\beta\right) + \left|x_n\right| sin\left(\theta_n - \theta'_\beta\right) = \left|x_p\right| \frac{\left|x_p\right| - \left|x_n\right| cos\left(\theta_n\right)}{\left|x'_\beta\right|} + \left|x_n\right| sin\left(\theta_n\right) \frac{\left|x_n\right| sin\left(\theta_n\right)}{\left|x'_\beta\right|} \\ &- \left|x_n\right| cos\left(\theta_n\right) \frac{\left|x_p\right| - \left|x_n\right| cos\left(\theta_n\right)}{\left|x'_\beta\right|} = \frac{\left|x_p\right|^2 + \left|x_n\right|^2 - 2\left|x_p\right|\left|x_n\right| cos\left(\theta_n\right)}{\left|x'_\beta\right|} = \left|x'_\beta\right|\end{aligned} \tag{29b}$$

The proposed transformation (12) with axes angles θ'_α and θ'_β selected according to (13) and (18) creates the time domain components x'_α and x'_β shifted by $\pi/2$, which may have different amplitudes. Therefore, further Park's transformation of these signals produces still oscillating components x'_d and x'_q in a rotating frame. To obtain non-oscillating components, the adequate scaling factors M_α, M_β for α' and β' axes are introduced. New components x'_α and x'_β have the same amplitudes. Finally, a new transformation (12) with unequal scales of the new frame axes takes the following form:

$$\boxed{\begin{bmatrix} x'_\alpha \\ x'_\beta \end{bmatrix} = \frac{1}{sin\left(\theta'_{\beta\alpha}\right)} \begin{bmatrix} M_\alpha sin\left(\theta'_\beta\right) & -M_\alpha cos\left(\theta'_\beta\right) \\ -M_\beta sin\left(\theta'_\alpha\right) & M_\beta cos\left(\theta'_\alpha\right) \end{bmatrix} \begin{bmatrix} x_\alpha \\ x_\beta \end{bmatrix}} \tag{30}$$

whereas scaling factors are described by the following equation:

$$\begin{bmatrix} M_\alpha \\ M_\beta \end{bmatrix} = \begin{bmatrix} \frac{\left|x\right|_{base}}{\left|x_\alpha\right|} \\ \frac{\left|x\right|_{base}}{\left|x_\beta\right|} \end{bmatrix} \tag{31}$$

and $|x|_{base}$ can be selected in different manners. One of the ways is to keep amplitudes $|x'_\alpha|$ and $|x'_\beta|$ equal to the higher of $|x_\alpha|, |x_\beta|$:

$$|x|_{base} = max\left\{|x_\alpha|, |x_\beta|\right\} \tag{32}$$

Another way is to keep the length of the x' vector in the new $\alpha'\beta'$ frame equal to the maximum length of vector x, represented in the natural $\alpha\beta$ frame. Then

$$\left|x\right|_{base} = \left|x\right|^{max} = \left|x_p\right| + \left|x_n\right| \tag{33}$$

The next case for the scaling factor is to obtain new x'_d and x'_q equal to the average values of x_d and x_q, respectively. Then

$$\left|x\right|_{base} = \left|x_p\right| \tag{34}$$

However, $|x|_{base}$ selected in these ways (32)–(34) seems to be useless for the current control system. Using the following equation seems to be the most interesting, because using this factor, we can assign the maximum amplitudes of unbalanced current vector components in a new frame, not to exceed the assumed maximum current in any phase:

$$\left|x\right|_{base} = max\left\{\left|x_a\right|, \left|x_b\right|, \left|x_c\right|\right\} = \left|x_{abc}\right|^{max} \tag{35}$$

To bring the x' vector to the frame rotating synchronously with a positive sequence vector, the Park's rotation transformation is used. Both transformations result in the following equation.

$$\begin{bmatrix} x'_d \\ x'_q \end{bmatrix} = \begin{bmatrix} cos(\theta_s) & sin(\theta_s) \\ -sin(\theta_s) & cos(\theta_s) \end{bmatrix} \begin{bmatrix} x'_\alpha \\ x'_\beta \end{bmatrix} = \boxed{\frac{1}{sin(\theta'_{\beta\alpha})} \begin{bmatrix} cos(\theta_s) & sin(\theta_s) \\ -sin(\theta_s) & cos(\theta_s) \end{bmatrix} \begin{bmatrix} M_\alpha sin(\theta'_\beta) & -M_\alpha cos(\theta'_\beta) \\ -M_\beta sin(\theta'_\alpha) & M_\beta cos(\theta'_\alpha) \end{bmatrix} \begin{bmatrix} x_\alpha \\ x_\beta \end{bmatrix}} \tag{36}$$

3. Assignment of Transformation Parameters

In order to apply the proposed transformation, the amplitudes and phase angles of $\alpha\beta$ vector components are needed. The SOGI structure (Patiño et al., 2015) presented in Fig. 3 for the x_α component of the vector x is used to find direct x_α^d and quadrature fundamental frequency x_α^q signals. The same is used for the x_β component of the vector.

As a result, four signals are obtained: x_α^d, x_α^q, x_β^d and x_β^q. Using these signals, $\alpha\beta$ components of the positive sequence vector $x_{p\alpha}$ and $x_{p\beta}$ can also be estimated. Calculation of all required amplitudes of vector components is shown in Fig. 4, whereas all trigonometric functions needed for the new transformation are described by the following equations:

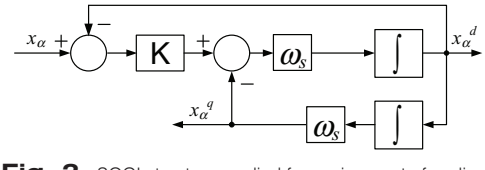

Fig. 3. SOGI structure applied for assignment of x_α direct and quadrature components.

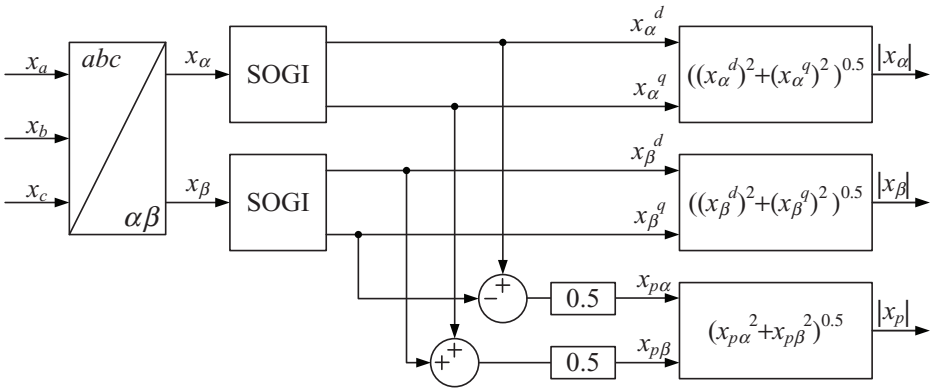

Fig. 4. Scheme presenting the method of determination of direct and quadrature signals of $\alpha\beta$ vector components, as well as amplitudes of $\alpha\beta$ components, and positive- and negative-sequence vectors.

$$sin\left(\theta'_\alpha\right)=\frac{x_{p\beta}x_\alpha^d-x_{p\alpha}x_\alpha^q}{\left|x_\alpha\right|\left|x_p\right|} \tag{37a}$$

$$cos\left(\theta'_\alpha\right)=\frac{x_\alpha^d x_{p\alpha}+x_\alpha^q x_{p\beta}}{\left|x_\alpha\right|\left|x_p\right|} \tag{37b}$$

$$sin\left(\theta'_\beta\right)=\frac{x_{p\beta}x_\beta^d-x_{p\alpha}x_\beta^q}{\left|x_\beta\right|\left|x_p\right|} \tag{37c}$$

$$cos\left(\theta'_\beta\right)=\frac{x_\beta^d x_{p\alpha}+x_\beta^q x_{p\beta}}{\left|x_\beta\right|\left|x_p\right|} \tag{37d}$$

$$sin\left(\theta'_{\beta\alpha}\right)=\frac{x_\beta^d x_\alpha^q-x_\alpha^d x_\beta^q}{\left|x_\alpha\right|\left|x_\beta\right|} \tag{37e}$$

Using trigonometric functions (37a–e), a modified transformation can be created, with which vector x containing positive and negative sequence is represented by $\alpha'\beta'$ components synchronized with positive-sequence $\alpha\beta$ components.

Amplitudes of $|x_a|,|x_b|$ and $|x_c|$ phase signals needed for scaling factor $|x|_{base}$ (35) can be assigned using inverse Clarke's transformation for each direct and quadrature phase signal x_a^d,x_b^d,x_c^d and x_a^q,x_b^q,x_c^q, respectively:

$$\begin{aligned} x_a^d &= x_\alpha^d \\ x_b^d &= -\frac{1}{2}x_\alpha^d+\frac{\sqrt{3}}{2}x_\beta^d \\ x_c^d &= -\frac{1}{2}x_\alpha^d-\frac{\sqrt{3}}{2}x_\beta^d \end{aligned} \tag{38}$$

$$x_a^q = x_\alpha^q$$
$$x_b^q = -\frac{1}{2}x_\alpha^q + \frac{\sqrt{3}}{2}x_\beta^q \tag{39}$$
$$x_c^q = -\frac{1}{2}x_\alpha^q - \frac{\sqrt{3}}{2}x_\beta^q$$

$$|x_a| = \sqrt{\left(x_a^d\right)^2 + \left(x_a^q\right)^2} = |x_\alpha| \tag{40}$$
$$|x_b| = \sqrt{\left(x_b^d\right)^2 + \left(x_b^q\right)^2}$$
$$|x_c| = \sqrt{\left(x_c^d\right)^2 + \left(x_c^q\right)^2}$$

4. Simulation Results of Non-Cartesian Frame Transformation Implementation

Simulation results of direct and quadrature components' calculation of $\alpha\beta$ signals, positive- and negative sequence components in the $\alpha\beta$ frame, as well as direct and quadrature components of phase signals are shown in Fig. 5. This is a confirmation of the method from Fig. 4 and equations (38)–(40). Results of the vector transformation in which the x' vector length equals the maximum amplitude of phase signals from Fig. 6a are shown in Fig. 6b. Fig. 6c presents vector components in dq and $d'q'$ frames. In a $d'q'$ frame, the vector components are constant.

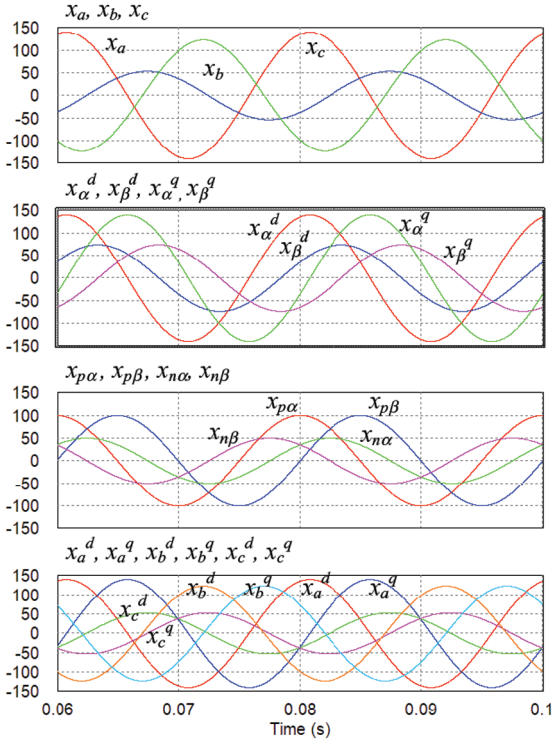

Fig. 5. Simulation results of a) unbalanced phase signals x_a, x_b, x_c, b) direct and quadrature components $x_\alpha^d, x_\alpha^q, x_\beta^d, x_\beta^q$ of $\alpha\beta$ signals, c) positive- and negative-sequence components $x_{p\alpha}, x_{p\beta}, x_{n\alpha}, x_{n\beta}$ in the $\alpha\beta$ frame and d) direct and quadrature phase signals $x_a^d, x_a^q, x_b^d, x_b^q, x_c^d, x_c^q$.

Simulation results have been obtained with the following data: $|x_p|=100$, $|x_n|=50$, initial angle of phase a of positive sequence vector $\pi/2$ and initial angle of phase a of negative sequence vector $\pi/4$. Sine and cosine functions of synchronous angle θ_s are calculated using (41ab). Simulation results of the combined transformation from $\alpha\beta$ to $\alpha'\beta'$ and next to $d'q'$ frame with consideration of 10% of fifth harmonic in the phase signals are shown in Fig. 7. It can be seen that new x'_d and x'_q components are constant, due to the harmonic filtration by SOGI filters used for determination of $\alpha\beta$ signals.

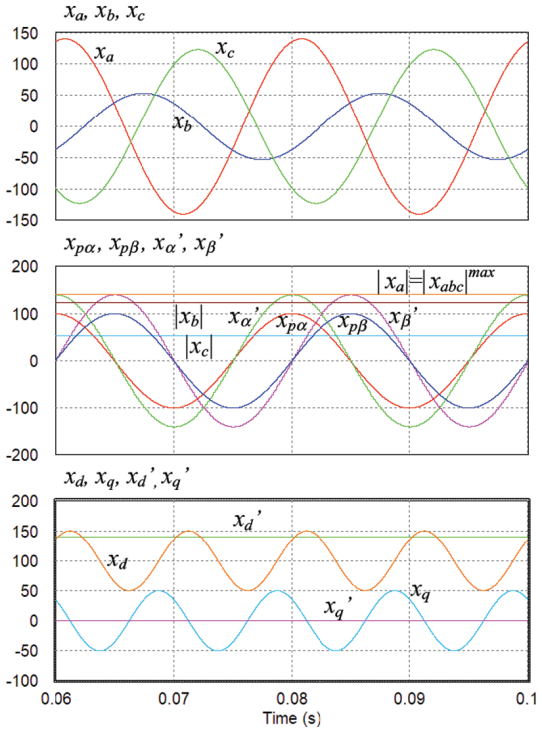

Fig. 6. Simulation results of a) unbalanced phase signals x_a, x_b, x_c, b) positive sequence $x_{p\alpha}, x_{p\beta}$, $\alpha'\beta'$ frame components x'_α, x'_β and determined amplitudes of phase signals $|x_a|, |x_b|, |x_c|$ and c) classic dq and new $d'q'$ frames components x_d, x_q, x'_d, x'_q when x_{base} is selected according to (35).

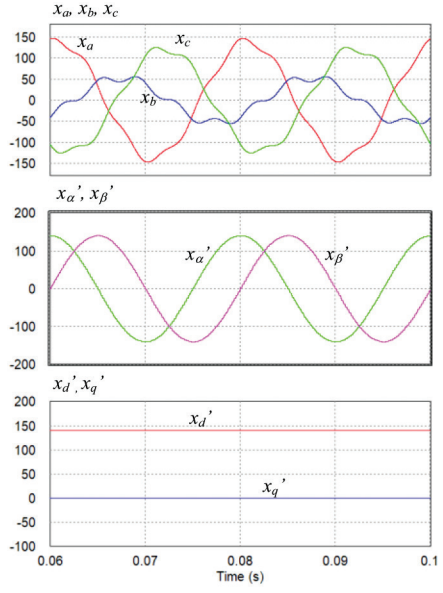

Fig. 7. Simulation results of a) unbalanced phase signals x_a, x_b, x_c, b) $\alpha'\beta'$ frame components x'_α, x'_β and c) $d'q'$ frame components x'_d, x'_q when the phase signals are distorted by 10% of fifth harmonic.

$$sin\left(\theta_s\right)=\frac{x_{p\beta}}{\left|x_p\right|} \tag{41a}$$

$$cos\left(\theta_s\right)=\frac{x_{p\alpha}}{\left|x_p\right|} \tag{41b}$$

5. Inverse Transformation

Let us write transformation (30) in the following form:

$$kx' = \mathbf{T}x \tag{42}$$

where $k = sin(\theta'_{\beta\alpha})$ and $\mathbf{T}$ is a transformation matrix.

Wishing to find x^i, when x' is known, we can write the following equation:

$$x^i = k\mathbf{T}^{-1}x' \tag{43}$$

where x^i is the vector obtained by inverse transformation from non-Cartesian frame $\alpha'\beta'$ to the natural $\alpha\beta$ frame, and

$$\mathbf{T}^{-1}=\frac{1}{\det\left(\mathbf{T}\right)}\mathbf{C}^{\mathbf{T}} \tag{44}$$

$$\det\left(\mathbf{T}\right)= M_\alpha M_\beta sin\left(\theta'_\beta\right)cos\left(\theta'_\alpha\right)- M_\alpha M_\beta cos\left(\theta'_\beta\right)sin\left(\theta'_\alpha\right)= M_\alpha M_\beta sin\left(\theta'_{\beta\alpha}\right) \tag{45}$$

$$\mathbf{C}^{\mathbf{T}}=\begin{bmatrix} M_\beta cos\left(\theta'_\alpha\right) & M_\alpha cos\left(\theta'_\beta\right) \\ M_\beta sin\left(\theta'_\alpha\right) & M_\alpha sin\left(\theta'_\beta\right) \end{bmatrix} \tag{46}$$

where $\mathbf{C}$ is a matrix of complements and $\mathbf{C}^{\mathrm{T}}$ is transposed $\mathbf{C}$.

From (43)–(46), an inverse transformation from $\alpha'\beta'$ to $\alpha\beta$ can be derived as follows:

$$x^i=\frac{k}{M_\alpha M_\beta sin\left(\theta'_{\beta\alpha}\right)}\begin{bmatrix} M_\beta cos\left(\theta'_\alpha\right) & M_\alpha cos\left(\theta'_\beta\right) \\ M_\beta sin\left(\theta'_\alpha\right) & M_\alpha sin\left(\theta'_\beta\right) \end{bmatrix}x' \tag{47}$$

The final form of the inverse transformation from non-Cartesian $\alpha'\beta'$ to the natural $\alpha\beta$ frame is

$$\boxed{\begin{bmatrix} x^i_\alpha \\ x^i_\beta \end{bmatrix}=\begin{bmatrix} \frac{1}{M_\alpha}cos\left(\theta'_\alpha\right) & \frac{1}{M_\beta}cos\left(\theta'_\beta\right) \\ \frac{1}{M_\alpha}sin\left(\theta'_\alpha\right) & \frac{1}{M_\beta}sin\left(\theta'_\beta\right) \end{bmatrix}\begin{bmatrix} x'_\alpha \\ x'_\beta \end{bmatrix}} \tag{48}$$

Transformation of the x' vector represented in the $d'q'$ frame to the natural $\alpha\beta$ frame needs two steps – the inverse Park's transformation from the $d'q'$ frame to non-Cartesian $\alpha'\beta'$ and next from non-Cartesian $\alpha'\beta'$ to the natural $\alpha\beta$, which together yield the following equation:

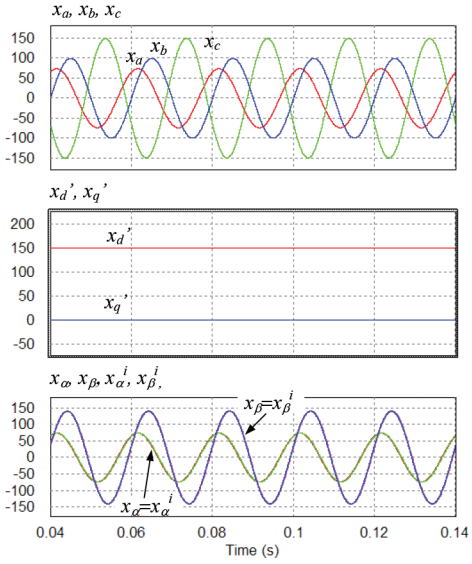

Fig. 8. Results of the inverse transformation from $d'q'$ to $\alpha\beta$ frame.

$$\begin{bmatrix} x_\alpha^i \\ x_\beta^i \end{bmatrix} = \begin{bmatrix} \frac{1}{M_\alpha}\cos(\theta'_\alpha) & \frac{1}{M_\beta}\cos(\theta'_\beta) \\ \frac{1}{M_\alpha}\sin(\theta'_\alpha) & \frac{1}{M_\beta}\sin(\theta'_\beta) \end{bmatrix} \begin{bmatrix} x'_\alpha \\ x'_\beta \end{bmatrix} \tag{49}$$

$$= \left[\begin{bmatrix} \frac{1}{M_\alpha}\cos(\theta'_\alpha) & \frac{1}{M_\beta}\cos(\theta'_\beta) \\ \frac{1}{M_\alpha}\sin(\theta'_\alpha) & \frac{1}{M_\beta}\sin(\theta'_\beta) \end{bmatrix} \begin{bmatrix} \cos(\theta_s) & -\sin(\theta_s) \\ \sin(\theta_s) & \cos(\theta_s) \end{bmatrix} \begin{bmatrix} x'_d \\ x'_q \end{bmatrix} \right]$$

The results of inverse $d'q'$ to $\alpha\beta$ transformation are shown in Fig. 8. It can be seen that x_α^i and x_β^i components, obtained as products of the inverse transformation, are almost equal to the original signals x_α and x_β, respectively. One sample delay, which is normal in digital signal processing, is caused by sampling frequency equal to 10 kHz.

6. Conclusion

The paper presents a theoretical analysis of a new transformation of unbalanced three-phase signals to the non-Cartesian frame in which the new axes positions are matched to imbalance of three-phase signals. As a consequence, the obtained signals in a new $\alpha'\beta'$ frame are shifted by $\pi/2$. The effect of adequate scaling factors is that the sinusoidal components have the same amplitudes; therefore, in a new frame, the vector is seen as balanced. A further transformation to the $d'q'$ frame creates constant vector components. The proposed combined transformations from $\alpha\beta$ to $\alpha'\beta'$ and next from $\alpha'\beta'$ to the $d'q'$ frame can be useful in modification of voltage-oriented vector control for power converters operating with unbalanced power grid. Using the proposed transformations, the control variables can be represented by constant components, which makes it possible to eliminate oscillatory terms. Finding the transformation parameters based on Fig. 4 and (37), (40) and (41) is relatively simple for application in typical digital signal processing platforms used in industries.

Acknowledgements

This work was supported by the National Science Centre (Poland) within the project granted on the basis of the decision number 2016/23/B/ST7/03942.

References

Abdeltawab, H. H. and Mohamed, Y. A. R. I. (2016). Robust Energy Management of a Hybrid Wind and Flywheel Energy Storage System Considering Flywheel Power Losses Minimization and Grid-Code Constraints. *IEEE Transactions on Industrial Electronics*, 63(7), pp. 4242–4254.

Abdel-Khalik, A. S., Hamad, M. S., Massoud, A. M. and Ahmed, S. (2018). Postfault Operation of a Nine-Phase Six-Terminal Induction Machine Under Single Open-Line Fault. *IEEE Transactions on Industrial Electronics*, 2, pp. 1084–1096.

Afshari, E., Moradi, G. R., Rahimi, R., Farhangi, B., Yang, Y., Blaabjerg, F. and Farhangi, S. (2017). Control Strategy for Three-Phase Grid-Connected PV Inverters Enabling Current Limitation Under Unbalanced Faults, *IEEE Transactions on Industrial Electronics*, 64(11), pp. 8908–8918.

Cheng, P., Nian, H. (2016). Direct Power Control of Voltage Source Inverter in a Virtual Synchronous Reference Frame During Frequency Variation and Network Unbalance. *IET Power Electronics*, 9, pp. 502–511.

Clarke, E. (1943). *Circuit Analysis of AC Power Systems–Symmetrical and Related Components*. Hoboken, NJ: John Wiley & Sons, vol. I.

Gałecki, A., Grzesiak, L., Ufnalski, B., Kaszewski, A. and Michalczuk, M. (2016). Anti-windup strategy for an LQ current controller with oscillatory terms for three-phase grid-tie VSCs in SMES systems. *Power Electronics and Drives*, 1(2), pp. 65–81

Gałecki, A., Michalczuk, M., Kaszewski, A., Ufnalski, B. and Grzesiak, L. M. (2018). Particle swarm optimization of the multioscillatory LQR for a three-phase grid-tie converter. *Przegląd Elektrotechniczny*, 94(6), pp. 43–48

Guo, X., Liu, W. and Lu, Z. (2017). Flexible Power Regulation and Current-Limited Control of the Grid-Connected Inverter Under Unbalanced Grid Voltage Faults. *IEEE Transactions on Industrial Electronics*, 64(9), pp. 7425–7432.

Guo, X. Q., Yang, Y. and Zhang X. (2018). Advanced Control of Grid-connected Current Source Converter under Unbalanced Grid Voltage Conditions. *IEEE Transactions on Industrial Electronics*, *Early Access*

Iwanski G. (2019). Virtual Torque and Power Control of a Three-Phase Converter Connected to an Unbalanced Grid with Consideration of Converter Current Constraint and Operation Mode. *IEEE Transactions on Power Electronics,* 34(4), pp. 3804–3818

Iwanski, G., Luszczyk, T. and Szypulski, M. (2017). Virtual-Torque-Based Control of Three-Phase Rectifier Under Grid Imbalance and Harmonics. *IEEE Transactions on Power Electronics,* 32(9), pp. 6836–6852.

Levi, E., Bojoi, R., Profumo, F., Toliyat, H. A. and Williamson, S. (2007). Multiphase induction motor drives - a technology status review. *IET Electric Power Applications*, 1, pp. 489–516.

Nian, H., Shen, Y., Yang, H. and Quan, Y. (2015). Flexible Grid Connection Technique of Voltage-Source Inverter Under Unbalanced Grid Conditions Based on Direct Power Control. *IEEE Transactions on Industry Applications,* 51, pp. 4041–4050.

Park, R. H. (1929). Two-Reaction Theory of Synchronous Machines Generalized Method of Analysis-Part I. *Transactions of the American Institute of Electrical Engineers*, 48(3), pp. 716–727.

Patiño, D. G., Erira, E. G. G., Rosero, E. E., Fuelagán, J. R. (2015). SOGI-FLL for synchronization and fault detection in an inverter connected to the grid. *Innovative Smart Grid Technologies Latin America (ISGT LATAM)*.

Rizo, M., Rodríguez, A., Rodríguez, F. J., Bueno, E. and Liserre, M. (2012). Different approaches of stationary reference frames saturators. In: 38th Annual Conference of the IEEE Industrial Electronics Society - *IECON.*

Rodriguez, P., Luna, A., Candela, I., Mujal, R., Teodorescu, R. and Blaabjerg, F. (2011). Multiresonant Frequency-Locked Loop for Grid Synchronization of Power Converters Under Distorted Grid Conditions. *IEEE Transactions on Industrial Electronics*, 58, pp. 127–138.

Xin, Z., Wang, X., Qin, Z., Lu, M., Loh, P. C. and Blaabjerg, F. (2016). An Improved Second-Order Generalized Integrator Based Quadrature Signal Generator. *IEEE Transactions on Power Electronics*, 31, pp. 8068–8073.